New Journal of Physics
The open access journal for physics

The Kondo effect of an adatom in graphene and its scanning tunneling spectroscopy

Lin Li[1,2], Yang-Yang Ni[1], Yin Zhong[1], Tie-Feng Fang[1] and Hong-Gang Luo[1,3,4]

[1] Center of Interdisciplinary Studies and Key Laboratory for Magnetism and Magnetic Materials of the Ministry of Education, Lanzhou University, Lanzhou 730000, People's Republic of China
[2] Department of Physics and Center of Theoretical and Computational Physics, The University of Hong Kong, Hong Kong, People's Republic of China
[3] Beijing Computational Science Research Center, Beijing 100084, People's Republic of China
E-mail: luohg@lzu.edu.cn

New Journal of Physics **15** (2013) 053018 (16pp)
Received 24 March 2013
Published 9 May 2013
Online at http://www.njp.org/
doi:10.1088/1367-2630/15/5/053018

Abstract. We study the Kondo effect of a single magnetic adatom on the surface of graphene. The unique linear dispersion relation near the Dirac points in graphene makes it easier for the magnetic atom to form a local magnetic moment, which simply means that the Kondo resonance can be observed in a wider parameter region than in the metallic host. Our study indicates that the Kondo resonance, whenever the chemical potential is tuned away from the Dirac points, can indeed occur ranging from the Kondo regime, to the mixed valence, even to the empty orbital regime defined in the conventional metal host. While the Kondo resonance appears as a sharp peak in the Kondo regime, it has a peak-dip structure and/or an anti-resonance in the mixed valence and empty orbital regimes, which result from the Fano resonance due to the significant background due to dramatic broadening of the impurity level in graphene. We also study the scanning tunneling microscopy (STM) spectra of the adatom and they show obvious particle–hole asymmetry when the chemical potential is tuned by the

[4] Author to whom any correspondence should be addressed.

gate voltages applied to the graphene. Finally, we explore the influence of the direct tunneling channel between the STM tip and the graphene on the Kondo resonance and find that the lineshape of the Kondo resonance is unaffected, which can be attributed to an unusually large asymmetry factor in graphene. Our study indicates that graphene is an ideal platform to systematically study Kondo physics and these results are useful to further stimulate relevant experimental studies on the system.

Contents

1. Introduction

The experimental realization of graphene [1, 2] composed of a monolayer of carbon atoms trigged a new wave of study of carbon-based materials, including both their fundamental physics and their applications [3–5]. The graphene possesses perfect two-dimensional massless Dirac fermion behaviors, and the valence and conduction bands touch at two inequivalent Dirac points K_- and K_+ at the corner of the Brillouin zone. Around the Dirac points the low-energy excitations are linear and the unique electronic structure leads to a number of unusual electronic correlation and transport properties of graphene [3–12].

For example, the localized magnetic moment on an adatom with inner shell electrons in graphene behaves quite differently to that in metals, a conventional Fermi liquid with a constant density of states near the Fermi surface. Anderson showed that in such a host the strongly interacting impurity ion can be in a magnetic state if the on-site interaction U is sufficiently large and/or the hybridization V between the impurity ion and the conduction electrons is sufficiently small [13, 14]. Explicitly, it is required that the energy of the single occupancy states ε_d is below the Fermi level μ but the energy of the double occupancy states, namely, $\varepsilon_d + U$, should be larger than μ. Moreover, the magnetic regime was found to be symmetric around $y = (\mu - \varepsilon_d)/U = 0.5$. For details one can refer to the phase diagram given by the well-known Anderson [13]. In contrast, when the host is graphene, the situation is dramatically different due to the linear density of states near the Dirac points [15–17]. Firstly, the magnetic phase diagram is not symmetric, it depends on the impurity level ε_d being above or below the Dirac points. The second and also most important difference is that the phase boundary is not symmetric around $y = 0.5$ in both cases. When ε_d is above the Dirac points, the magnetic state extends to $y < 0$, which means that even the impurity level is located above the Fermi energy, and it is possible that the localized magnetic moment exists. This is quite different to that in a usual metallic host.

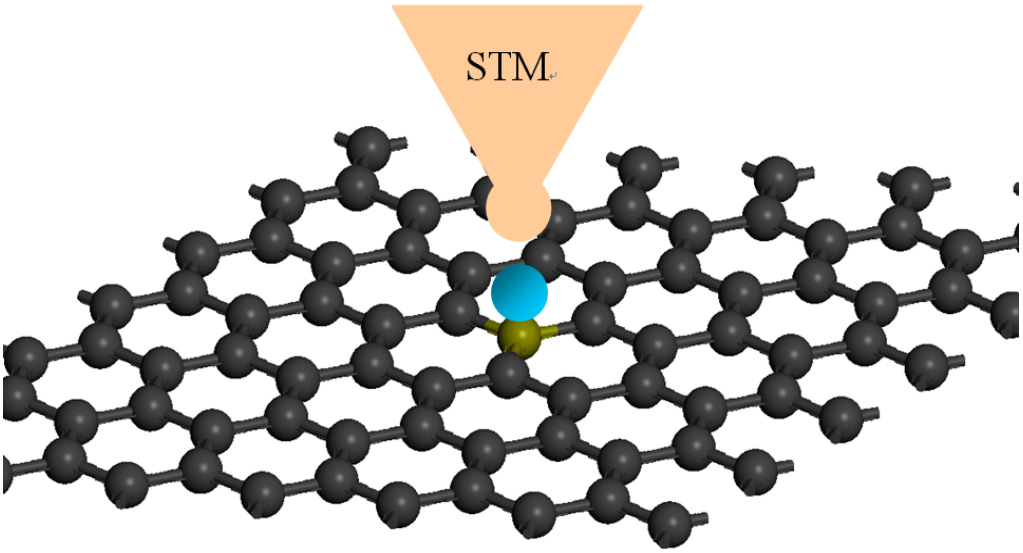

Figure 1. Schematic diagram of the STM measurement of a magnetic adatom absorbed on the top of a carbon atom site.

In the other case, in which ε_d is below the Dirac points, the phase boundary extends to $y > 1$, which means that even the impurity is in the double occupancy state, and it can be magnetized. It was realized that all these unusual features are due to the linear dispersion of the graphene around the Dirac points, and the impurity level is broadened dramatically by hybridization to cross the Fermi level [15].

A direct consequence of the much wider magnetic regime is that the Kondo effect in graphene [18] may exist in a wider parameter regime than that in the usual metallic host, in which the Kondo effect only exists in the Kondo regime, namely, $\epsilon_d/\Gamma \ll -0.5$ [19], where Γ is the effective tunneling coupling between the impurity and conduction electrons. Moreover, it is also interesting to explore what effect the dramatic broadening of the impurity level has on the Kondo physics. This motivates us to study the Kondo effect of an adatom on the surface of a graphene sheet in a systematic way.

In this work the system we are interested in consists of the adatom, the graphene and the tip on the top of the adatom, as shown in figure 1. As the first step, we explore the intrinsic equilibrium Kondo effect of the adatom as the conduction sea of electrons is limited to the graphene. The Kondo physics of the adatom generally depends on its explicit positions on the surface of the graphene, which show rich electronic structures [11, 20–22]. When the adatom is absorbed on the top of carbon atom, the situation is quite simple since the orbital degrees of freedom are not involved in this case. However, when the adatom is located at the center of the honeycomb, a high symmetry position, the adatom hybridizes with the carbon atoms in both sublattices [11, 20, 22–25], thus the orbital degrees of freedom are involved which complicates the Kondo physics. The magnetic impurity substitution of the carbon atom [26, 27] or an adatom positioned on top of non-hexagonal rings [28] also proposes many interesting physical properties. However, our interest here is to discuss the essential difference in Kondo physics between the metallic bath with a constant density of states and the Dirac electron bath with linear low-energy dispersion. In order to clarify this issue, the first simple case is enough and we will leave the complicated cases for future study.

When the Fermi energy is near the Dirac points, the Kondo effect is absent since a critical coupling strength must be satisfied for developing the Kondo effect [10, 18, 29–32], as also obtained by using the numerical renormalization group calculations in the gapless Kondo and/or Anderson models [33–35]. Once the Fermi energy is tuned to be away from the Dirac points, whether it is below or above the Dirac points, the Kondo resonance is found to exist in a wide parameter regime ranging from the Kondo regime to the mixed valence regime, and even to the empty orbital regime[5]. This is consistent with our intuition since the localized magnetic moment exists in a very wide parameter regime. When the system is in the Kondo regime, the Kondo resonance manifests as a sharp peak. This peak appears weaker and weaker when the impurity level becomes deeper and deeper. This is understandable since the broadening of the impurity level becomes weak due to the low density of states of the graphene near the Dirac points. When the system is in the mixed valence or empty orbital regimes, the Kondo resonance develops. However, it does not show a sharp peak but a peak-dip structure, even an anti-resonance, which is a typical Fano resonance behavior [36, 37].

In the next step, we consider a normal tip on the top of the adatom and the aim is to study the scanning tunneling microscopy (STM) spectra of the Kondo resonance of the adatom in graphene. We first turn off the direct tunneling between the tip and the graphene. The Kondo resonance shows asymmetric behavior that depends on the position of the Fermi energy, namely, it is above or below the Dirac points. Moreover, the Kondo temperature strongly but asymmetrically depends on the explicit position of the Fermi energy which is in agreement with reports in the literature [30, 31, 38]. Subsequently, we turn on the direct tunneling between the tip and the graphene to study its influence on the lineshape of the Kondo resonance, which is also a more realistic case. It is somehow surprising that the lineshape is almost unaffected by the additional direct channel. This result in fact originates from the unusually large asymmetry factor in graphene.

The paper is organized as follows. In section 2 we take the single-impurity Anderson model to describe the adatom on the surface of the graphene and derive the transport formula by Keldysh non-equilibrium Green's function theory. In section 3 we solve numerically the equations obtained, in a self-consistent way, and discuss explicitly the Kondo effect in various situations including the cases of (i) the adatom plus the graphene, (ii) the adatom plus the graphene plus the tip and (iii) the STM spectra with the direct channel between the tip and the graphene. Finally, section 4 is devoted to a brief summary.

2. Model and formalism

The Hamiltonian of a magnetic adatom on graphene with an STM tip consists of the following terms:

$$H = H_{\rm d} + H_{\rm g} + H_{\rm dg} + H_{\rm t} + H_{\rm dt} + H_{\rm tg}, \tag{1}$$

where

$$H_{\rm d} = \sum_{\sigma} \varepsilon_{\rm d} d_{\sigma}^{\dagger} d_{\sigma} + U\, d_{\sigma}^{\dagger} d_{\sigma} d_{\bar{\sigma}}^{\dagger} d_{\bar{\sigma}} \tag{2}$$

[5] To compare conventionally with the results in the metal host, these regimes are defined as in the metal host [14]. However, in the graphene both the impurity level and the linewidth are renormalized and one can classify the parameter regimes according to the Wilson's renormalization group.

describes the magnetic adatom with the impurity level $\varepsilon_{\rm d}$ and the on-site interaction U [13]. Here $d_\sigma^\dagger$ (d_σ) is a creation (annihilation) operator of localized electrons on a magnetic adatom with spin σ ($=\uparrow,\downarrow$) and $\bar{\sigma}=-\sigma$. The second term in equation (1) is the tight-banding Hamiltonian describing graphene, which can be written in momentum space as

$$H_{\rm g}=-t\sum_{k\sigma}(\eta_k a_{k\sigma}^\dagger b_{k\sigma}+{\rm H.c.}), \tag{3}$$

$a_{k\sigma}^\dagger$ ($a_{k\sigma}$) and $b_{k\sigma}^\dagger$ ($b_{k\sigma}$) are creation (annihilation) operators of electrons in sublattices A and B, respectively. t is the hopping energy between the nearest-neighbor carbon atoms, $\eta_k=\sum_{i=1}^{3}{\rm e}^{{\rm i}\vec{k}\cdot\vec{r}_i}$ with $\vec{r}_1=a\vec{x}$, $\vec{r}_2=-\frac{a}{2}\vec{x}+\frac{\sqrt{3}a}{2}\vec{y}$, $\vec{r}_3=-\frac{a}{2}\vec{x}-\frac{\sqrt{3}a}{2}\vec{y}$ and $a\approx 1.42\,\text{Å}$ is the carbon–carbon spacing [4]. The low-energy transport properties of graphene are mostly determined by the nature of the spectrum around the Dirac points $K_\pm$ at the corners of the Brillouin zone, where the dispersion is $\varepsilon_k\approx\pm\upsilon_{\rm F}|k|$, the sign $+(-)$ corresponds to the conduction (valence) band, and $\upsilon_{\rm F}=3ta/2$ ($\approx 10^6\,{\rm m\,s^{-1}}$) is the Fermi velocity of Dirac electrons. The tip Hamiltonian is described by a normal metal

$$H_{\rm t}=\sum_{k\sigma}\xi_k t_{k\sigma}^\dagger t_{k\sigma}, \tag{4}$$

where $t_{k\sigma}^\dagger$ ($t_{k\sigma}$) represents the creation (annihilation) of an electron with energy ξ_k on the tip. The Hamiltonians

$$H_{\rm dg}=\sum_{k\sigma}(V_{ka\sigma}a_{k\sigma}^\dagger+V_{kb\sigma}b_{k\sigma}^\dagger)d_\sigma+{\rm H.c.} \tag{5}$$

and

$$H_{\rm dt}=\sum_{k\sigma}(V_{kt\sigma}t_{k\sigma}^\dagger d_\sigma+{\rm H.c.}) \tag{6}$$

represent electrons tunneling from a magnetic adatom to graphene and to an STM tip, respectively. $V_{ka\sigma}$ ($V_{kb\sigma}$) is the electron tunneling amplitude between the magnetic adatom and sublattice A (B), and $V_{kt\sigma}$ is the tunneling amplitude between the magnetic adatom and the STM tip. If the adatom is adsorbed above the carbon atom in sublattice A, thus $V_{ka\sigma}=V_{kg\sigma}$ and $V_{kb\sigma}=0$ or in sublattice B, thus $V_{ka\sigma}=0$ and $V_{kb\sigma}=V_{kg\sigma}$. The direct tunneling Hamiltonian between graphene and the STM tip is described by

$$H_{\rm tg}=\sum_{kk'\sigma}T_{\rm tg}(t_{k\sigma}^\dagger b_{k'\sigma}+t_{k\sigma}^\dagger a_{k'\sigma})+{\rm H.c.}, \tag{7}$$

where $T_{\rm tg}$ is the hopping amplitude between the STM tip and the graphene sheet.

In the steady state, the current from the STM tip to the graphene sheet can be calculated by the time-dependent occupancy number

$$\begin{aligned}I&=-\frac{e}{2}(\langle\dot{N}_{\rm t}\rangle-\langle\dot{N}_{\rm g}\rangle)=-\frac{{\rm i}e}{2\hbar}\left\langle\left[H,\left(N_{\rm t}-N_{\rm g}\right)\right]\right\rangle\\&=-\frac{e}{\hbar}{\rm Re}\sum_{k\sigma}\left(V_{{\rm kg}\sigma}^*G_{\sigma,{\rm gk}\sigma}^<(t,t')-V_{{\rm kt}\sigma}^*G_{\sigma,{\rm tk}\sigma}^<(t,t')\right)\\&\quad-\frac{2e}{\hbar}{\rm Re}\sum_{kk'\sigma}T_{\rm tg}^*G_{{\rm tk}\sigma,{\rm g}k'\sigma}^<(t,t'),\end{aligned} \tag{8}$$

where $N_t = \sum_{k\sigma} t^\dagger_{k\sigma} t_{k\sigma}$ and $N_g = \sum_{k\sigma} c^\dagger_{k\sigma} c_{k\sigma}$. Here we use $c^\dagger_{k\sigma}(c_{k\sigma})$ to denote the electron creation (annihilation) operator in the graphene sheet. The current is related to the lesser Green's functions defined as $G^<_{\sigma,tk\sigma}(t,t') = i\langle t^\dagger_{k\sigma}(t') d_\sigma(t)\rangle$, $G^<_{\sigma,gk\sigma}(t,t') = i\langle c^\dagger_{k\sigma}(t') d_\sigma(t)\rangle$ and $G^<_{tk\sigma,gk'\sigma}(t,t') = i\langle c^\dagger_{k'\sigma}(t') t_{k\sigma}(t)\rangle$. These Green's functions can be calculated by the equations of motion (EOM) approach based on non-equilibrium Green's functions theory. For detail one can refer to [39].

To simplify, we assume that the tunneling amplitudes $V_{kg\sigma} = V_g$ and $V_{kt\sigma} = V_t$ are independent on energy and spin. After some straightforward derivations, one can obtain the current formula

$$I = \frac{ie}{h}\sum_\sigma \int \{(G^r_\sigma(\varepsilon) - G^a_\sigma(\varepsilon))[\Gamma_t(\varepsilon) f_t(\varepsilon) - \Gamma_g(\varepsilon) f_g(\varepsilon)] + (\Gamma_t(\varepsilon) - \Gamma_g(\varepsilon)) G^<_\sigma(\varepsilon)\} d\varepsilon$$

$$+\frac{2e}{h}\int (f_t(\varepsilon) - f_g(\varepsilon)) \left[\Pi(\varepsilon) - \Phi(\varepsilon)\sum_\sigma \mathrm{Im}\,(G^r_\sigma(\varepsilon))\right] d\varepsilon, \tag{9}$$

where $G^{<,r,a}_\sigma(\varepsilon)$ is the Fourier transformation of the time-order Green's function $G^{<,r,a}_\sigma(t,t')$ defined by $G^<_\sigma(t,t') = i\langle d^\dagger_\sigma(t') d_\sigma(t)\rangle$, $G^{r(a)}_\sigma(t,t') = \mp i\theta(\pm t \mp t')\langle\{d_\sigma(t), d^\dagger_\sigma(t')\}\rangle$. $\Gamma_g(\varepsilon) = \pi|V_g|^2\rho_g(\varepsilon)$ and $\Gamma_t(\varepsilon) = \pi|V_t|^2\rho_t(\varepsilon)$ are the couplings between the magnetic adatom and the graphene, and between the magnetic adatom and the tip, respectively. $\Pi(\varepsilon) = \pi|T_{tg}|^2\rho_t(\varepsilon)\rho_g(\varepsilon)$ corresponds to hopping from the tip to graphene and vice versa. $\Phi(\varepsilon) = \sqrt{\pi\Pi(\varepsilon)\Gamma_g(\varepsilon)\Gamma_t(\varepsilon)}$ is related to the interference between the different tunneling channels. $\rho_g(\varepsilon)$ and $\rho_t(\varepsilon)$ are the density of states of graphene and the STM tip, respectively. The density of states for the tip is simplified with a constant $\rho_t(\varepsilon) = 1/2D$, and the density of states for graphene can be evaluated with $\rho_g(\varepsilon) = \Theta(D - |\varepsilon|)|\varepsilon|/D^2$ [25]. Here D is the half-width of the conduction band and $\Theta(x)$ is the Heaviside step function. For convenience, we take $\Gamma_g(\varepsilon) = \Gamma_0|\varepsilon|/D$ where $\Gamma_0 = \pi|V_g|^2/D$. $f_g(\varepsilon)$ and $f_t(\varepsilon)$ are the Fermi distribution functions of graphene and the STM tip. The non-equilibrium Kondo effect can be obtained by differential conductance near the Fermi level. Thus, our final task, to calculate the current, is to solve the Green's functions involved.

Equations for the retarded Green's functions and the lesser Green's functions can be derived by the Schwinger–Keldysh perturbation formalism [40–43] and are given by, respectively,

$$G^r_\sigma(\varepsilon) = g^r_d(\varepsilon)\left(1 + \langle\langle[d_\sigma, H_I]; d^\dagger_\sigma\rangle\rangle^r_\varepsilon\right), \tag{10}$$

$$G^<_\sigma(\varepsilon) = g^<_d(\varepsilon)\left(1 + \langle\langle[d_\sigma, H_I]; d^\dagger_\sigma\rangle\rangle^a_\varepsilon\right) + g^r_d(\varepsilon)\langle\langle[d_\sigma, H_I]; d^\dagger_\sigma\rangle\rangle^<_\varepsilon, \tag{11}$$

where $g^r_d(\varepsilon) = 1/(\varepsilon - \varepsilon_d + i0^+)$ and $g^<_d(\varepsilon) = i\pi f(\varepsilon)\delta(\varepsilon - \varepsilon_d)$ are the non-interacting retarded and lesser Green's functions for the isolated magnetic adatom. In the above expressions the $H_I = U d^\dagger_\sigma d_\sigma d^\dagger_{\bar\sigma} d_{\bar\sigma} + H_{dg} + H_{dt}$ includes the on-site Coulomb repulsion term on the adatom and the tunneling terms. While the first term will introduce higher-order Green's functions contained into $\langle\langle[d_\sigma, H_I]; d^\dagger_\sigma\rangle\rangle^{r(a,<)}_\varepsilon$ by using Zubarev notations [44], the remaining two terms only lead to the hybridization effect. Furthermore, the derivation of the EOM of the higher-order Green's function will also introduce more higher-order Green's functions, which have to be truncated in order to close the hierarchy of the EOM of the successive Green's functions. Here we truncate this hierarchy of EOM by using Lacroix's scheme [45], which is shown to be enough to capture

the Kondo resonance, even at zero temperature [45, 46]. Since the derivation is standard we do not go into the detail but directly write down the Green's functions in the infinite-U limit as follows:

$$G^r_\sigma(\varepsilon) = \frac{1 - \langle n_{\bar\sigma}\rangle - A_{\bar\sigma}(\varepsilon)}{\varepsilon - \varepsilon_{\rm d} - \Sigma(\varepsilon)\,(1 - A_{\bar\sigma}(\varepsilon)) - B_{\bar\sigma}(\varepsilon)} \tag{12}$$

and

$$G^<_\sigma(\varepsilon) = G^r_\sigma(\varepsilon)\left(\Sigma^<(\varepsilon) + \Sigma^<_I(\varepsilon)\right) G^a_\sigma(\varepsilon). \tag{13}$$

Here the self-energy $\Sigma(\varepsilon) = \frac{-{\rm i}\Gamma(\varepsilon) - \frac{\varepsilon\Gamma_{\rm g}(\varepsilon)}{\pi|\varepsilon|}\ln\left(D^2/\varepsilon^2 - 1\right) - \Phi(\varepsilon) - (\Phi(\varepsilon))^*}{1+\pi\Pi(\varepsilon)}$, $\Gamma(\varepsilon) = \Gamma_{\rm g}(\varepsilon) + \Gamma_{\rm t}(\varepsilon)$, the lesser self-energy $\Sigma^<(\varepsilon) = \frac{{\rm i}\Xi_1(\varepsilon)+\Omega(\varepsilon)}{1+\pi\Pi(\varepsilon)}$ and $\Sigma^<_I(\varepsilon) = \frac{B^<_{\bar\sigma}(\varepsilon) - A^<_{\bar\sigma}(\varepsilon)\left(G^a_\sigma(\varepsilon)^{-1} + \Sigma(\varepsilon)\right)}{1 - \langle n_{\bar\sigma}\rangle - A_{\bar\sigma}(\varepsilon)}$, the average of occupation $\langle n_{\bar\sigma}\rangle = -\frac{1}{\pi}\int \frac{\Xi_1(\varepsilon)}{\Gamma(\varepsilon)}{\rm Im}\,(G^r_{\bar\sigma}(\varepsilon))\,{\rm d}\varepsilon$ and

$$A_{\bar\sigma}(\varepsilon) = \frac{1}{\pi}\int \frac{g(\varepsilon,\varepsilon')\,(\Xi_1(\varepsilon') + {\rm i}\Omega(\varepsilon'))\,(G^r_{\bar\sigma}(\varepsilon'))^*}{1+\pi\Pi(\varepsilon')}\,{\rm d}\varepsilon', \tag{14}$$

$$\begin{aligned} B_{\bar\sigma}(\varepsilon) = {} & \frac{1}{\pi}\int g(\varepsilon,\varepsilon')\Xi_1(\varepsilon'){\rm d}\varepsilon' \\ & + \frac{\rm i}{\pi}\int g(\varepsilon,\varepsilon')(\Xi_2(\varepsilon') + \Xi_3(\varepsilon'))(G^r_{\bar\sigma}(\varepsilon'))^*\,{\rm d}\varepsilon' \\ & + \frac{1}{\pi}\int \frac{g(\varepsilon,\varepsilon')\Xi_1(\varepsilon')\Phi(\varepsilon')(G^r_{\bar\sigma}(\varepsilon'))^*}{1+\pi\Pi(\varepsilon')}{\rm d}\varepsilon', \end{aligned} \tag{15}$$

$$A^<_{\bar\sigma}(\varepsilon) = \frac{{\rm i}\Xi_1(\varepsilon){\rm Re}\,(G^r_{\bar\sigma}(\varepsilon)) + {\rm i}\Omega(\varepsilon){\rm Im}(G^r_{\bar\sigma}(\varepsilon))}{1+\pi\Pi(\varepsilon)}, \tag{16}$$

$$\begin{aligned} B^<_{\bar\sigma}(\varepsilon) = {} & {\rm i}\Xi_1(\varepsilon) + {\rm i}(\Xi_2(\varepsilon) + \Xi_3(\varepsilon)){\rm Im}\,(G^r_{\bar\sigma}(\varepsilon)) \\ & - {\rm i}\Xi_1(\varepsilon)\frac{\Phi(\varepsilon){\rm Im}\,(G^r_{\bar\sigma}(\varepsilon))}{1+\pi\Pi(\varepsilon)}, \end{aligned} \tag{17}$$

where $g(\varepsilon,\varepsilon') = 1/(\varepsilon - \varepsilon' + {\rm i}0^+)$, $\Omega(\varepsilon) = \Phi(\varepsilon)f_{\rm g}(\varepsilon) + (\Phi(\varepsilon))^* f_{\rm t}(\varepsilon)$, $\Xi_1(\varepsilon) = f_{\rm g}(\varepsilon)\Gamma_{\rm g}(\varepsilon) + f_{\rm t}(\varepsilon)\Gamma_{\rm t}(\varepsilon)$, $\Xi_2(\varepsilon) = f_{\rm g}(\varepsilon)\Gamma_{\rm g}(\varepsilon)\Gamma_{\rm g}(\varepsilon) + f_{\rm t}(\varepsilon)\Gamma_{\rm t}(\varepsilon)\Gamma_{\rm t}(\varepsilon)$, $\Xi_3(\varepsilon) = \Gamma_{\rm g}(\varepsilon)\Gamma_{\rm t}(\varepsilon)(f_{\rm gt}(\varepsilon) + f_{\rm tg}(\varepsilon))$ with $f_{\rm gt}(\varepsilon) = f_{\rm g}(\varepsilon)(1 - f_{\rm t}(\varepsilon))$. At the hand of the above expressions, we can calculate numerically the Green's function $G^r_\sigma(\varepsilon)$—and $G^a_\sigma(\varepsilon) = (G^r_\sigma(\varepsilon))^*$ in a self-consistent way—and further the lesser Green's function $G^<_\sigma(\varepsilon)$. Finally, we obtain the current I by equation (9).

3. Numerical results and discussions

In the following numerical calculation, several input parameters are tuned in order to study the system in different physical situations. The atomic level $\epsilon_{\rm d}$ is changed to study the different regimes ranging from the Kondo regime to the mixed valence regime, even to the empty orbital regime [19]. The chemical potential μ of graphene can be tuned by a gate-voltage, which makes the Fermi level located at ($\mu = 0$), above ($\mu > 0$) or below ($\mu < 0$) the Dirac points. The different chemical potentials will lead to quite different physics, as shown below. The voltage bias $V_{\rm sd}$ is also applied between the STM tip and the graphene sheet to calculate the

differential conductance. For convenience, we take Γ_0 as the units of energy in the calculations. In a systematic way, we first calculate the Kondo effect of the adatom plus the graphene when the STM tip is absent. The aim is to explore the influence of the linear dispersion around the Dirac points on the Kondo effect and compare it with the adatom on a normal metal surface. Subsequently, we consider the influence of the STM tip and explore the Kondo resonance when both the normal metal and the graphene are coupled to the adatom. Finally, we turn on the direct channel between the STM tip and the graphene and check its effect on tunneling spectroscopy, which is more closely related to experiment.

3.1. Kondo effect of the adatom without the scanning tunneling microscopy (STM) tip

In order to explore the effect of the linear dispersion around the Dirac points, we first study the system composed of the magnetic adatom plus the graphene and neglect the STM tip. As pointed out by Uchoa *et al* [15], it is easier for the magnetic impurity to form a local moment on the surface of the graphene than in the normal metal host. This conclusion has a direct consequence: that one can observe the Kondo resonance in a wider parameter region for the former than the latter. This is really true as shown in figures 2 and 3 where we show the local density of states of the adatom given by $\rho_{\rm d}(\varepsilon) = -\frac{1}{\pi}{\rm Im}\, G^r_\sigma(\varepsilon)$. In figure 2 we consider $\mu = 0.5\Gamma_0$, namely, the Fermi level is above the Dirac points. We change the atomic level from the empty orbital regime, as shown in figure 2(a) to the Kondo regime (see figure 2(f)). Around the Fermi level the local density of states show special features, i.e. Kondo resonance, although their shapes are quite different. In the Kondo regimes, the Kondo resonance appears as a sharp peak around the Fermi level, but one should notice that with increasing atom level the peak becomes gradually asymmetric, which is quite obvious in figure 2(d) for $\varepsilon_{\rm d} = 0$. Continuing to change the atomic level to $\varepsilon_{\rm d} = 0.5\Gamma_0$, the Kondo resonance has a typical dip structure. Finally, as we move the atomic level to the empty orbital regimes, the Kondo effect manifests continuously as a dip structure, which becomes weaker and weaker with increasing atomic level, as clearly seen from the inset of figures 2(a) and (b). The dip structure originates from the Fano resonance, as explained briefly below.

In the absence of the STM tip, namely, $\Gamma_t(\varepsilon) \equiv 0$, equation (12) is rewritten approximately as near the Fermi level

$$G_\sigma(\varepsilon) \approx \frac{1 - \langle n_{\bar\sigma}\rangle}{\varepsilon - \varepsilon_{\rm d} + {\rm i}\Gamma_{\rm g}(\varepsilon) - B_{\bar\sigma}(\varepsilon)}. \tag{18}$$

Here for simplicity we neglect $A_{\bar\sigma}$ since $B_{\bar\sigma}$ already captures the essential physics of Kondo resonance [45]. In addition, the real part of the self-energy $\Sigma(\varepsilon)$ is also omitted. Equation (18) can be further rewritten approximately as

$$G(\varepsilon) \approx G^0(\varepsilon) + G^0(\varepsilon)\, T(\varepsilon)\, G^0(\varepsilon), \tag{19}$$

where $G^0(\varepsilon) = \frac{1-n/2}{\varepsilon - \varepsilon_{\rm d} + {\rm i}\Gamma_{\rm g}(\varepsilon)}$ and $T(\varepsilon) = \frac{B(\varepsilon)}{1-n/2}$. Here for simplicity the spin index is dropped and $n = \langle n_\uparrow\rangle + \langle n_\downarrow\rangle$. From equation (19), the impurity density of states reads

$$\rho(\varepsilon) = \rho_0(\varepsilon) - \pi\rho_0^2(\varepsilon)[(q_{\rm d}^2 - 1){\rm Im}\, T(\varepsilon) - 2q_{\rm d}{\rm Re}\, T(\varepsilon)], \tag{20}$$

where $q_{\rm d} = -{\rm Re}\, G^0(\varepsilon)/{\rm Im}\, G^0(\varepsilon)$ and $\rho_0(\varepsilon) = -{\rm Im}\, G^0(\varepsilon)/\pi$. Generally, $T(\varepsilon)$ is a complicated function of ε but the Kondo resonance (if it exists) is a unique feature of $T(\varepsilon)$ near the Fermi

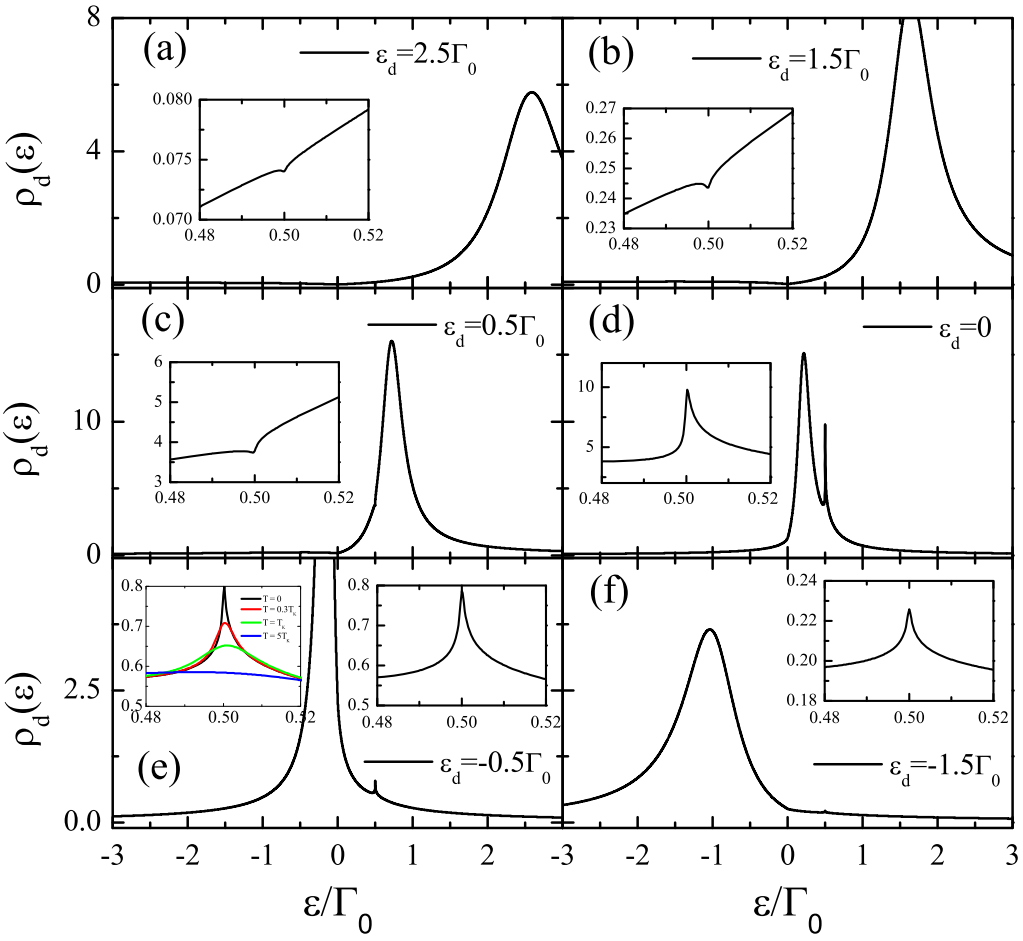

Figure 2. The Kondo resonance in the density of states of the magnetic adatom on graphene with different atomic levels ranging from the empty orbital regime to the Kondo regime. From (a) to (f) the atomic level is $\epsilon_{\rm d} = 2.5\Gamma_0$, $1.5\Gamma_0$, $0.5\Gamma_0$, 0, $-0.5\Gamma_0$, $-1.5\Gamma_0$. The inset in each panel is an enlarged view around the Kondo resonance. The chemical potential is $\mu = 0.5\Gamma_0$, the temperature $T = 0.00005\Gamma_0$ and the half-bandwidth $D = 5\Gamma_0$. The left inset in (e) shows the temperature dependence of the Kondo resonance.

level in the Anderson impurity system. Thus $T(\varepsilon)$ is given approximately by

$$T(\varepsilon) \approx \frac{\Gamma_{\rm K}}{\pi\rho_0(\varepsilon)} \frac{1}{\varepsilon - \varepsilon_{\rm K} + {\rm i}\Gamma_{\rm K}}, \tag{21}$$

where $\varepsilon_{\rm K}$ is the position of the Kondo resonance and $\Gamma_{\rm K}$ is its width. Inserting (21) into (20) and defining $\tilde{\varepsilon} = (\varepsilon - \varepsilon_{\rm K})/\Gamma_{\rm K}$, one obtains

$$\rho(\varepsilon) \approx \rho_0(\varepsilon_{\rm K}) \frac{(\tilde{\varepsilon} + q_{\rm d})^2}{\tilde{\varepsilon}^2 + 1}, \tag{22}$$

which is a standard form of the Fano resonance [36, 37].

The lineshape of the Kondo resonance is determined by $q_{\rm d}$. In the Kondo regime ($|\varepsilon_{\rm d} - \varepsilon_{\rm F}| \gg \Gamma_{\rm g}(\varepsilon_{\rm F})$, thus $|q_{\rm d}| \gg 1$) the broadening of the impurity level is quite weak around

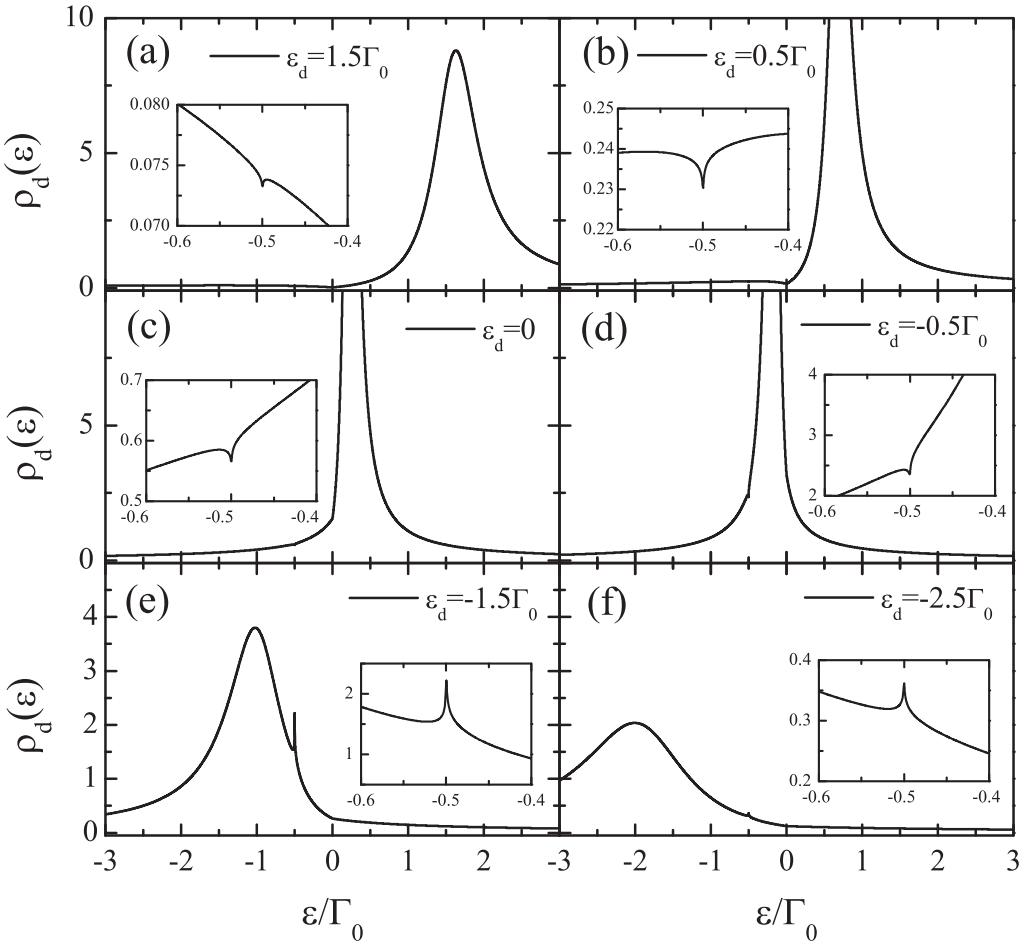

Figure 3. The same as figure 2 but for $\mu = -0.5\Gamma_0$. From (a) to (f) the atomic level is $\varepsilon_d = 1.5\Gamma_0, 0.5\Gamma_0, 0, -0.5\Gamma_0, -1.5\Gamma_0, -2.5\Gamma_0$.

ε_F so the Kondo resonance shows as a symmetric peak. When the system approaches the mixed valence regime ($|\varepsilon_d - \varepsilon_F| \lesssim \Gamma_g(\varepsilon_F)$, thus $|q_d| \lesssim 1$), the broadening of the impurity level becomes more and more sizeable and as a result, the Kondo peak distorts gradually due to interference, and finally it becomes a dip structure, as shown in figures 2(a) and (b), where the system is already in the empty orbital regime in the sense of the metallic host. That is to say, the Kondo effect can exist in a wider parameter region in the graphene host than that in the metallic host. The essential reason for this is that the impurity level is broadened extensively due to the linear density of states of the graphene around the Dirac points. Therefore, the adatom on the surface of the graphene provides an ideal platform to study the Kondo effect in various parameter spaces. The temperature behavior of the peak around the Fermi level shown in the left inset in figure 2(e) confirms that the peak observed is Kondo resonance since it becomes gradually broader with increasing temperature and disappears completely when the temperature is greater than the Kondo temperature T_K [38]. The same physics has been observed when the Fermi level is below the Dirac points, as shown in figures 3(a)–(f).

To confirm the above observation, we compare the local density of states around the Fermi level for the adatom on graphene and on a metal surface in the empty orbital regime, as

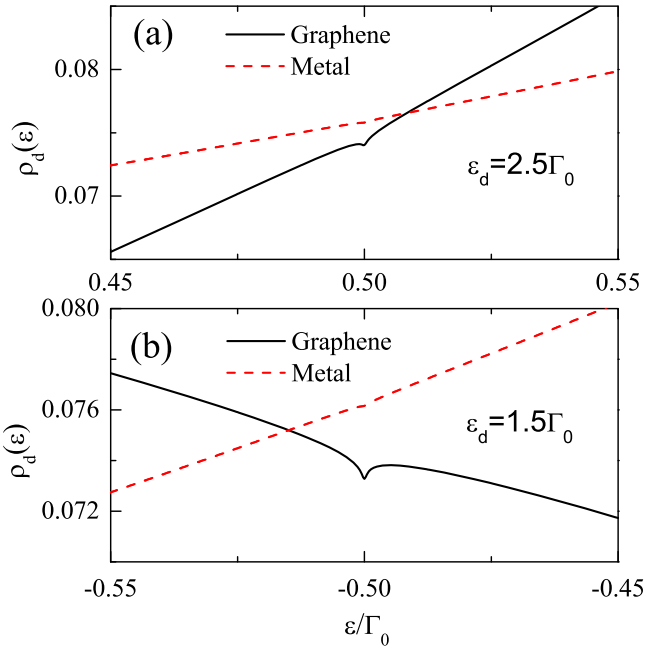

Figure 4. Comparison between the density of states around the Fermi level in the empty orbital regime for the metallic (red dashed lines) and the graphene (solid lines) hosts. (a) $\mu = 0.5\Gamma_0$, $\varepsilon_d = 2.5\Gamma_0$, and (b) $\mu = -0.5\Gamma_0$, $\varepsilon_d = 1.5\Gamma_0$.

shown in figure 4. For a metal host, one cannot observe any feature, which is in contrast to the graphene, where an obvious dip exists. The result that the chemical potential is above or below the Dirac points is true in both cases.

As mentioned above, the results presented are obtained by the EOM up to the Lacroix's approximation level [45]. For the single impurity Anderson model the impurity density of states in the Kondo, mixed-valence and even the empty orbital regimes have been calculated by using the EOM, which are qualitatively consistent with those obtained by the numerical renormalization group [37]. To further confirm the validity of this method in the case of a graphene host, we calculate the impurity occupation as a function of the impurity energy level, as shown in figure 5 for three different chemical potentials. It is noticed that the occupation increases more rapidly for $\mu > 0$ than for $\mu < 0$. This observation is qualitatively consistent with that obtained by the numerical renormalization group for a similar model but with finite U [16].

3.2. Kondo effect of the adatom with the STM tip

When the STM tip is considered, the adatom couples with two baths. One is the STM tip which is a normal metal with a constant density of states, as studied in conventional Kondo physics. One can also model the STM tip by a semi-infinite chain of atoms, but the essential physics does not change. The other is the graphene which has a linear density of states around the Dirac points. We first study the non-equilibrium Kondo effect in this case. Thus, we neglect the direct channel between the STM tip and the graphene. In the calculations, the coupling between the adatom and tip is taken with $\Gamma_t = 0.1\Gamma_0$. Figure 6 shows the differential conductance around

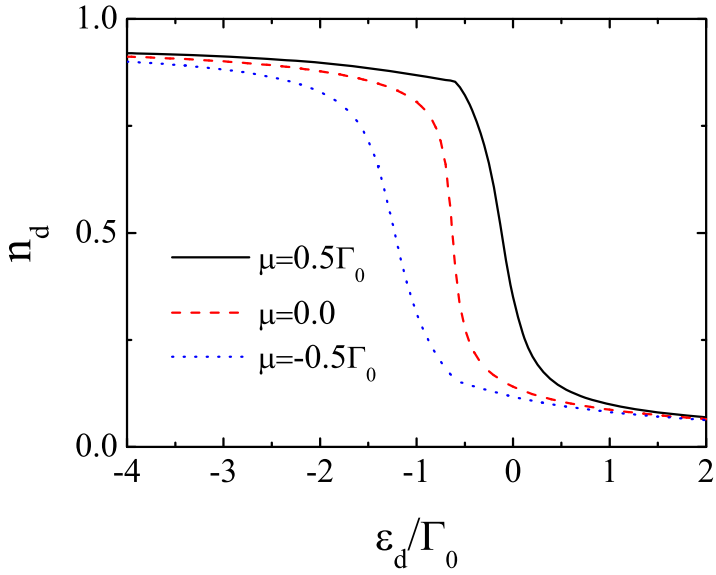

Figure 5. The impurity occupation as a function of the impurity level for three different chemical potentials $\mu = 0.5\Gamma_0$ (solid line), 0 (dashed line) and $0.5\Gamma_0$ (dotted line).

the zero bias. When the chemical potential μ is tuned to meet the Dirac points, the curve at the zero bias does not show any Kondo peak, which is a consequence of the zero density of states at the Dirac points. This is consistent with that reported in the literature [18, 29–32]. In this case, a critical coupling between the adatom and the conduction electron is required. When the chemical potential μ is tuned to be away from the Dirac points, either above or below the Dirac points, the zero-bias resonance peak occurs, which shows the Kondo effect [30, 31]. When the chemical potential is below the Dirac points, the larger $|\mu|$ is, the wider the peak is. This is easy to understand since a larger μ means a larger density of states at the side of the graphene. When μ is above the Dirac points, the width of the Kondo resonance remains almost unchanged (see figure 6(c)), which can also be obtained from the chemical-potential dependent Kondo temperature [38]. However, when μ is below the Dirac points, the Kondo temperature T_K shows obvious dependence on μ. As a result, the Kondo temperature is obviously asymmetric, which is also consistent with that reported in the literature [30, 38]. This is due to the fact of the particle–hole asymmetry in graphene. In addition, one also notes that in both cases the curves show a kink when the bias scans through the Dirac points.

3.3. Scanning tunneling spectroscopy with direct channel

In this section we discuss the scanning tunneling spectroscopy of the adatom on the surface of graphene by switching on the direct tunneling channel between the STM tip and the graphene, a more realistic case in experiments. Due to the additional direct channel, one may expect that the STM spectroscopy should be changed dramatically, led by the interference between the direct and the indirect channels, as usually observed in a system with the adatom on the surface of the normal metals [47]. However, the result is somewhat surprising, as shown in figure 7. In comparison with the spectroscopy without the direct channel, except for the amplitudes, the

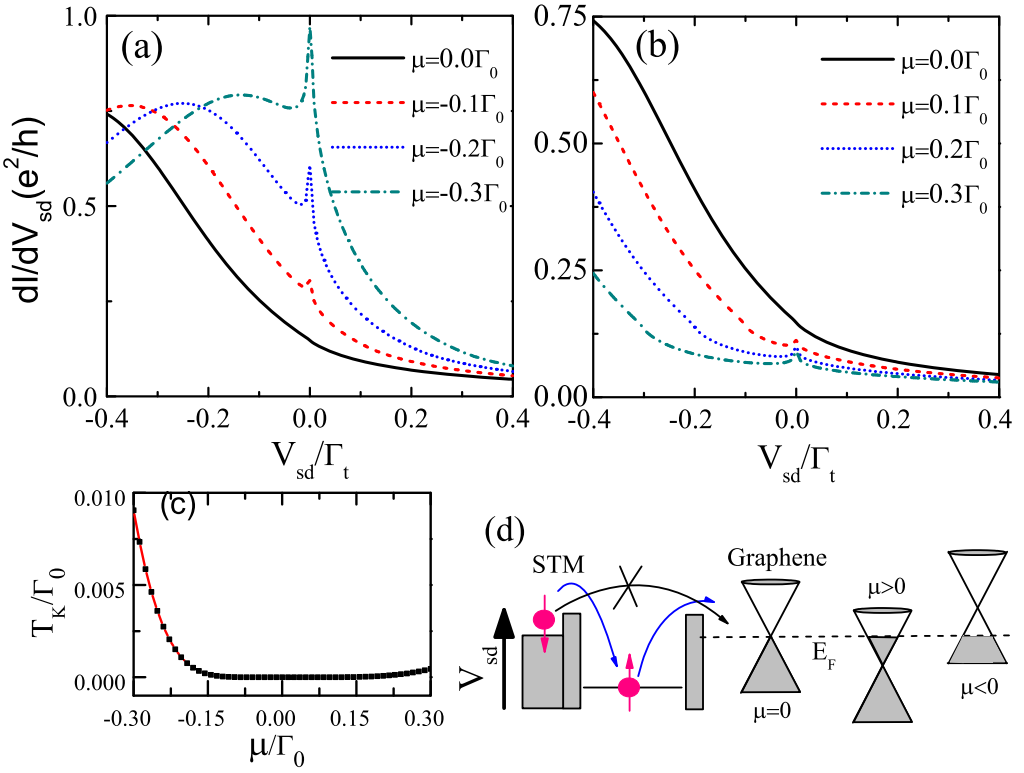

Figure 6. The Kondo resonance around the zero bias varies with the chemical potential (a) $\mu < 0$ and (b) $\mu > 0$. (c) The Kondo temperature T_k versus the chemical potential μ. The other parameters used are $\epsilon_d = -\Gamma_0$ where $\Gamma_t = 0.1\Gamma_0$, $T_{tg} = 0$ and $D = 5\Gamma_0$. Panel (d) shows schematically the cotunneling processes with the chemical potentials $\mu < 0$ and $\mu > 0$, respectively.

shape almost remains unchanged for both $\mu > 0$ and $\mu < 0$. To check the underlying physics of this result, let us recall the Fano resonance theory [36]. In the STM case, due to the adatom scattering and its interference with the direction channel, the differential conductance of the conduction electron can be written as [37]

$$\frac{dI}{dV} \propto (q^2 - 1)\mathrm{Im}\, G(\varepsilon) - 2q\mathrm{Re}\, G(\varepsilon), \tag{23}$$

where $G(\varepsilon)$ denotes the adatom Green's function and $q \approx -\mathrm{Re}\, g(\varepsilon)/\mathrm{Im}\, g(\varepsilon)$ is the Fano asymmetry factor. Here $g(\varepsilon)$ is the graphene Green's function with $\mathrm{Re}\, g(\varepsilon) = (\varepsilon/D^2)\ln|\varepsilon^2/(D^2 - \varepsilon^2)|$ and $\mathrm{Im}\, g(\varepsilon) = -\pi|\varepsilon|/D^2\Theta(D - |\varepsilon|)$. Thus the q factor is $2\,\mathrm{sgn}(\mu)/\pi\,\ln|\mu|/D$ near the Fermi level [25]. For graphene, $D \sim 6\,\mathrm{eV}$ [48] and if $|\mu|$ is maximally in the order of 0.1 eV, so $|q| \gtrsim 6$. That means that the first term in equation (23) dominates the second term, and as a result, dI/dV has almost the same profile as $\mathrm{Im}\, G(\varepsilon)$, the local density of states of the adatom. This is the reason that the shape of the Kondo resonance around the zero bias is almost the same whether the direct channel is switched on or off. This picture also explains the result obtained by Cornaglia *et al* [16] that the STM spectrum is almost the same irrespective of whether the matrix element for the tunneling of an electron from the tip to the conduction band is present or absent. Experimentally, one can test the prediction by manipulating a transition metal atom like Co on top of graphene using the STM tip and measuring its local spectral signatures, which is

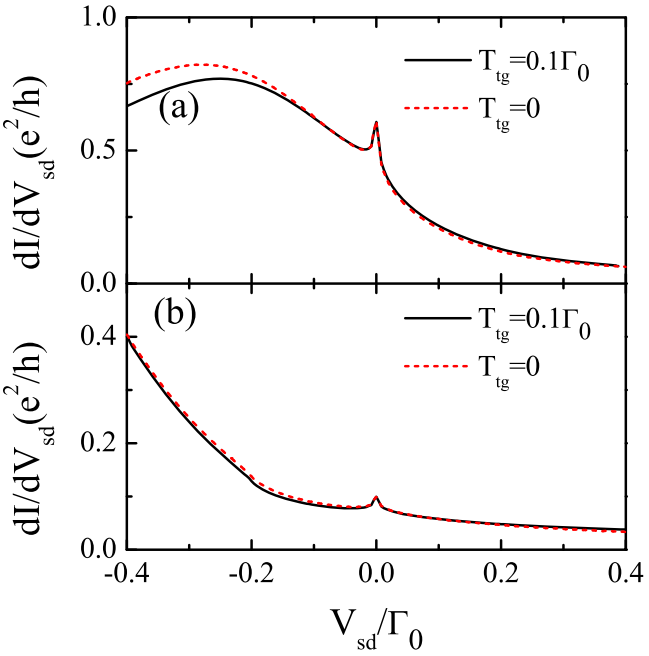

Figure 7. The Kondo resonance around the zero bias with and without the direct tunneling T_{tg} channel for two cases (a) $\mu = -0.2\Gamma_0$ and (b) $\mu = 0.2\Gamma_0$. We take $\varepsilon_d = -\Gamma_0$ and $T_{tg} = 0, 0.1\Gamma_0$. The other parameters used are the same as figure 6.

feasible in the present experimental setup [49], as has been carried out on a conventional metal surface [47].

4. Summary

In summary, we systematically study the Kondo effect of a magnetic adatom on the surface of graphene and its STM spectra. The main conclusion is that the Kondo resonance can exist in a wide parameter region ranging from the Kondo regime to the mixed valence regime, and even to the empty orbital regime. In the mixed valence or the empty orbital regimes the Kondo resonance shows a special lineshape due to the Fano resonance, since in these regimes the broadening of the impurity level provides a significant background. The STM spectra have a particle–hole asymmetry when the chemical potential in graphene is tuned by the gate voltages. Furthermore, it is found that the direct tunneling channel between the STM tip and graphene has no obvious effect on the lineshape of the Kondo resonance around the zero bias, which is a consequence of the unusually large asymmetry factor in the graphene host. The rich behavior of the Kondo resonance obtained indicate that the graphene is an ideal platform to study Kondo physics and these results are useful to further stimulate relevant experimental work in this system.

Acknowledgments

Support from CMMM of Lanzhou University, NSFC, PCSIRT (grant no. IRT1251), the national program for basic research and the fundamental research funds for the central universities of China is acknowledged.

References

[1] Novoselov K S, Geim A K, Morozov S V, Jiang D, Zhang Y, Dubonos S V, Grigorieva I V and Firsov A A 2004 *Science* **306** 666

[2] Novoselov K S, Geim A K, Morozov S V, Jiang D, Katsnelson M I, Grigorieva I V, Dubonos S V and Firsov A A 2005 *Nature* **438** 197

[3] Beenakker C W J 2008 Colloquium: Andreev reflection and Klein tunneling in graphene *Rev. Mod. Phys.* **80** 1337

[4] Castro Neto A H, Guinea F, Peres N M R, Novoselov K S and Geim A K 2009 *Rev. Mod. Phys.* **81** 109

[5] Peres N M R 2010 *Rev. Mod. Phys.* **82** 2673

[6] Kotov V N, Uchoa B, Pereira V M, Neto A H C and Guinea F 2012 *Rev. Mod. Phys.* **84** 1067

[7] Peres N M R, Guinea F and Castro Neto A H 2006 *Phys. Rev.* B **73** 125411

[8] Ziegler K 2006 *Phys. Rev. Lett.* **97** 266802

[9] Nomura K and MacDonald A H 2007 *Phys. Rev. Lett.* **98** 076602

[10] Zhuang H-B, Sun Q-F and Xie X C 2009 *Europhys. Lett.* **86** 58004

[11] Jacob D and Kotliar G 2010 *Phys. Rev.* B **82** 085423

[12] Dell'Anna L 2010 *J. Stat. Mech.* P01007

[13] Anderson P W 1961 *Phys. Rev.* **124** 41

[14] Hewson A C 1993 *The Kondo Problem to Heavy Fermions* (Cambridge: Cambridge University Press)

[15] Uchoa B, Kotov V N, Peres N M R and Castro Neto A H 2008 *Phys. Rev. Lett.* **101** 026805

[16] Cornaglia P S, Usaj G and Balseiro C A 2009 *Phys. Rev. Lett.* **102** 046801

[17] Hu F M, Ma T, Lin H-Q and Gubernatis J E 2011 *Phys. Rev.* B **84** 075414

[18] Sengupta K and Baskaran G 2008 *Phys. Rev.* B **77** 045417

[19] Goldhaber-Gordon D, Göres J, Kastner M A, Shtrikman H, Mahalu D and Meirav U 1998 *Phys. Rev. Lett.* **81** 5225

[20] Uchoa B, Yang L, Tsai S W, Peres N M R and Castro Neto A H 2009 *Phys. Rev. Lett.* **103** 206804

[21] Zhu Z-G, Ding K-H and Berakdar J 2010 *Europhys. Lett.* **90** 67001

[22] Uchoa B, Rappoport T G and Castro Neto A H 2011 *Phys. Rev. Lett.* **106** 016801

[23] Saha K, Paul I and Sengupta K 2010 *Phys. Rev.* B **81** 165446

[24] Wehling T O, Balatsky A V, Katsnelson M I, Lichtenstein A I and Rosch A 2010 *Phys. Rev.* B **81** 115427

[25] Wehling T O, Dahal H P, Lichtenstein A I, Katsnelson M I, Manoharan H C and Balatsky A V 2010 *Phys. Rev.* B **81** 085413

[26] Krasheninnikov A V, Lehtinen P O, Foster A S, Pyykko P and Nieminen R M 2009 *Phys. Rev. Lett.* **102** 126807

[27] Santos E J G, Ayuela A and Sanchez-Portal D 2010 *New J. Phys.* **12** 053012

[28] Cretu O, Krasheninnikov A V, Rodriguez-Manzo J A, Sun L, Nieminen R M and Banhart F 2010 *Phys. Rev. Lett.* **105** 196102

[29] Cassanello C R and Fradkin E 1996 *Phys. Rev.* B **53** 15079

[30] Vojta M, Fritz L and Bulla R 2010 *Europhys. Lett.* **90** 27006

[31] Fritz L and Vojta M 2013 *Rep. Prog. Phys.* **76** 032501

[32] Maiti M, Saha K and Sengupta K 2012 *Int. J. Mod. Phys.* B **26** 1242002

[33] Withoff D and Fradkin E 1990 *Phys. Rev. Lett.* **64** 1835

[34] Ingersent K 1996 *Phys. Rev.* B **54** 11936
Gonzalez-Buxton C and Ingersent K 1998 *Phys. Rev.* B **57** 14254

[35] Gonzalez-Buxton C and Ingersent K 1996 *Phys. Rev.* B **54** 15614

[36] Fano U 1961 *Phys. Rev.* **124** 1866

[37] Luo H G, Xiang T, Wang X Q, Su Z B and Yu L 2004 *Phys. Rev. Lett.* **92** 256602
Luo H G, Xiang T, Wang X Q, Su Z B and Yu L 2006 *Phys. Rev. Lett.* **96** 019702

[38] Zhu Z-G and Berakdar J 2011 *Phys. Rev.* B **84** 165105

[39] Jauho A P, Wingreen N S and Meir Y 1994 *Phys. Rev.* B **50** 5528
[40] Mahan G D 1993 *Many-Particle Systems* 3rd edn (New York: Plenum) pp 561–7
[41] Niu C, Lin D L and Lin T H 1999 *J. Phys.: Condens. Matter* **11** 1511
[42] Świrkowicz R, Barnaś J and Wilczyński M 2003 *Phys. Rev.* B **68** 195318
[43] Krawiec M and Wysokiński K I 2004 *Supercond. Sci. Technol.* **17** 103–112
[44] Zubarev D N 1960 *Usp. Fiz. Nauk* **71** 71
Zubarev D N 1960 *Sov. Phys.—Usp.* **3** 320
[45] Lacroix C 1981 *J. Phys. F: Met. Phys.* **11** 2389
[46] Luo H-G, Ying Z-J and Wang S-J 1999 *Phys. Rev.* B **59** 9710
[47] Madhavan V, Chen W, Jamneala T, Crommie M F and Wingreen N S 1998 *Science* **280** 567
[48] Wehling T O, Balatsky A V, Katsnelson M I, Lichtenstein A I, Scharnberg K and Wiesendanger R 2007 *Phys. Rev.* B **75** 125425
[49] Brar V W *et al* 2010 *Nature Phys.* **7** 43